Available online at www.sciencedirect.com
SCIENCE DIRECT
International Journal of Psychophysiology 61 (2006) 262 – 278
INTERNATIONAL JOURNAL OF PSYCHOPHYSIOLOGY
www.elsevier.com/locate/ijpsycho

Amplitude modulation of gamma band oscillations at alpha frequency produced by photic driving

David B. Chorlian *, Bernice Porjesz, Henri Begleiter

Neurodynamics Laboratory, Department of Psychiatry, SUNY/HSCB, 450 Clarkson Ave., Brooklyn, NY, United States

Received 19 April 2005; received in revised form 1 November 2005; accepted 2 November 2005
Available online 27 December 2005

Abstract

Gamma band response to visual stimulation in humans has been observed to have both burst and resonance properties. Amplitude modulation of gamma activity at low frequencies has been seen in rat hippocampus and modeled in a number of forms. Significant amplitude modulation ($p=0.05$) of 33 Hz gamma frequency activity at the frequency of an 8 1/3 Hz photic driving stimulus, which also produced strong alpha entrainment, was observed in 67% of the channels in 42 human subjects. Similar amplitude modulation was found at a range of frequencies from greater than 50 Hz to about 28 Hz. The peak of the gamma amplitude modulation curve trailed the peak of the alpha signal by 25 to 30 ms, corresponding to a phase difference of 150° to 180°. The phase consistency of the gamma signal, measured across comparable times of the alpha signal, was least at the minimum amplitude modulation, and largest at the maximum. Although there was no consistent overall relation between the gamma amplitude and alpha amplitude, peak gamma amplitude values were consistently higher during post-target-stimulus alpha suppression, which occurs about 300–750 ms subsequent to stimulus presentation, than they were at the time of maximum alpha activity during the immediate post-stimulus period. It is hypothesized that there is an interaction between the alpha and gamma generating systems, in which gamma triggers alpha activity and is subsequently inhibited by it, thus producing the observed amplitude modulation. The transition from dark to light of the photic driving stimulus begins a phase resetting process in the gamma system and a concomitant burst of gamma activity; this produces an activation in the alpha system, similar to that found in the P1–N1 response in evoked potential experiments, and a subsequent inhibition of gamma production.

Keywords: Gamma; Alpha; Photic driving; Amplitude modulation

1. Introduction

Low frequency information can be conveyed by amplitude modulation of a high frequency carrier wave. In the neurophysiological context, high frequency neural activity, such as gamma band oscillations, can be modulated to convey information about stimuli which have a lower frequency temporal structure. A number of research studies have reported stimulus elicited gamma band oscillations in the visual cortex of different species of animals, and suggest that they may provide the high frequency carrier band for the transmission of low frequency stimulus characteristics (Samonds and Bonds, 2005; Nase et al., 2003; Friedman-Hill et al., 2000). Recent work by Eckhorn et al. (2005a,b) and Volgushev et al. (2003, 2004) explicitly mention amplitude modulation of gamma oscillations in the visual cortex as a mechanism of information transmission. In human evoked-potentials with visual stimuli, gamma-band activity is observed as a precursor of lower frequency activity (see below for a detailed discussion). Thus it is possible that the gamma amplitude modulation reported here, which represents the entrainment of the gamma amplitude to a photic driving stimulus, is an example of this mode of information transmission. In addition, the particular characteristics of the gamma amplitude modulation indicate an interaction between gamma and alpha oscillatory activity in the human visual system. It is important to note that the entrainment of the gamma amplitude to the photic driving

* Corresponding author. Tel.: +1 718 270 2231.
E-mail address: chorlian@cns.hscbklyn.edu (D.B. Chorlian).

0167-8760/$ - see front matter © 2005 Elsevier B.V. All rights reserved.
doi:10.1016/j.ijpsycho.2005.11.002

stimulus which our experimental paradigm elicited is not the same as the entrainment of the gamma band *oscillation* to the photic driving stimulus. These are distinct phenomena; each could occur without the other.

As will become clear, the gamma activity examined here is primarily a sensory phenomenon; its functional significance is not in question. However, the numerous experiments whose primary concern is the functional significance of gamma, in particular, those that illustrate relations between activity in gamma and lower frequency bands, will be relevant to the interpretation of our results. In the literature concerning the functional significance of gamma and other oscillatory activity, it is hypothesized that there are different functions for oscillations of different frequencies (von Stein and Sarnthein, 2000). Drawing on data from a number of evoked potential experiments, one hypothesis is that the higher frequency (28–80 Hz) gamma oscillations produced shortly after stimulus presentation are primarily involved with the sensory systems, and that subsequent lower frequency oscillations are involved with more complex functioning, from perception to higher cognition (Karakas and Basar, 1998; Karakas et al., 2001; Basar et al., 2001a). Only a relatively few experiments have been designed to test the ongoing interaction of the sensory and cognitive systems by eliciting steady-state evoked potentials concurrently with those evoked by response to aperiodic stimuli (Morgan et al., 1996; Müller and Hillyard, 2000); such experiments would enable the study of the ongoing relation between high and low frequency oscillatory systems. Many evoked potential experiments have produced gamma activity in humans in response to visual stimulation (Tomberg, 1999; Senkowski and Herrmann, 2002; Bakhtazad et al., 2003; Busch et al., 2004; Spencer et al., 2003, 2004). Two papers have reported gamma–theta coupling in memory related experiments (Burgess and Ali, 2002; Schack et al., 2002), and there is a single report of coupling between gamma and low frequency activity in a sensory experiment in humans (Bruns and Eckhorn, 2004). Parra et al. (2003) report entrainment of gamma in response to low frequency visual stimulation. In lower mammals, a number of researchers have reported coupling between higher and lower frequencies (Schanze and Eckhorn, 1997; von Stein et al., 2000). Volgushev et al. (2003, 2004) report gamma amplitude modulation at low frequencies in visual cortex cells in adult cats in response to visual stimulation. In vitro experiments and corresponding network simulations have yielded significant results regarding the interaction of high and low frequency systems (Whittington et al., 2000; White et al., 2000; Tiesinga and Sejnowski, 2004; Csicsvari et al., 2003; Somogyi and Klausberger, 2004; Káli and Freund, 2004). The in vitro experiments have dealt with the hippocampal system, not the visual system, so their relevance may be limited in explaining the phenomena reported here. However, the model offered by Káli and Freund (2004) of the interaction between CA1 pyramidal cells and oriens-lacunosum moleculare interneurons provides for a reciprocal relation between high and low frequency activity. Theoretical work regarding the coupling of frequencies in the visual system is limited (Azizi et al., 1996; Sewards and Sewards, 1999).

With regard to gamma production, particularly its temporal characteristics, it is plausible that early gamma activity elicited by visual stimulus presentation has an onset which ranges between 75 and 150 ms subsequent to stimulus presentation, and has a duration of approximately 75 ms. In addition, it seems that gamma activity is not purely sensory, but is affected by stimulus significance (Senkowski and Herrmann, 2002; Spencer et al., 2004). In an experiment designed to determine the effect on gamma production of a variety of sensory features, Busch et al. (2004) elicits gamma activity whose time course is directly determined by stimulus duration. Under those particular experimental conditions, a visual stimulus which is at least 150 ms in duration will elicit gamma both to the ON and OFF phases, with the response to the OFF occurring about 100 ms after the cessation of the stimulus. On the other hand, a stimulus at least as short as 50 ms will elicit only a single gamma burst, which is explained as the merging of the responses to the ON and OFF phases. This indicates that gamma production is as much a response to a change of state (transition), in this case the appearance of the stimulus, as to the state itself, in this case the characteristics of the stimulus. This result is crucial to the interpretation of our data. How these bursts of gamma activity are related to lower frequency activity is not discussed by Busch et al. (2004).

In order to discriminate between the activities of the neural systems and to determine the amplitude and phase relations in the associated oscillatory systems, we designed an experiment to provide both a continual and periodic stimulation of the sensory system and an aperiodic, intermittent stimulation of higher perceptual and cognitive systems. This means that aperiodic changes in the activity of the oscillatory components are the result of changes in perceptual and cognitive activity, not simply in sensory processing, while periodic changes related to the periodicity of the background sensory stimulus must be related primarily to the sensory system. The object of the experiment is to cause the entrainment of alpha EEG activity by photic driving, and to affect the entrainment by imposing a visual oddball task. (By entrainment we mean that the oscillation recorded from the scalp mimics the periodicity of the stimulus.) In an earlier paper we gave a preliminary analysis of the alpha activity which showed both amplitude and frequency modulation effects in response to both target and non-target stimuli in the visual oddball task (Chorlian et al., 2003). In this paper we focus on the interaction of the gamma and alpha systems. In order to characterize this interaction we use several measures of phase consistency to quantify the phase relations of the gamma and alpha oscillatory systems.

2. Experimental design and data collection

2.1. Experimental design

The experiment consists of a background visual stimulus that elicits alpha band photic driving with a superimposed visual oddball paradigm. The oddball task requires the subject to press a button whenever an infrequently occurring target foreground stimulus first appears on the screen. In the

experiment, entrainment is produced through the use of a flashing background stimulus on which the non-flashing foreground stimulus appears. The background stimulus is a square on the video screen that alternates between white and black, each occurring for 60 ms, continuously throughout the approximately 12.5 min of the experiment; this produces the 8 1/3 Hz photic driving. The foreground stimulus is either the letter 'A' or the numeral '5' presented in red. The '5' occurs in 13% of the trials in a pseudo-random sequence, and the subject is directed to push a button as soon as it appears on the screen. For the purpose of analysis, the experiment is divided into trials, 3.25 s in length, such that the background stimulus is the same at each corresponding sample point in the different trials. In each trial either the 'A' or the '5' appears on the screen for the duration of the trial. The foreground stimulus changes only on the appearance of the target stimulus in place of the non-target stimulus, and on the replacement of the target stimulus by the non-target stimulus 3.25 s later. The interval between successive target stimuli ranges from 6.5 to 30 s. Trials are classified by being a target trial or by their distance from the immediately preceding target trial.

2.1.1. Subjects

The control sample ($n=42$; mean age 27.8 years; S.D. 5.7 years, 25 males, 17 females) were individuals who responded to newspaper advertisements or notices posted in the SUNY Health Science Center. All subjects were screened using a questionnaire regarding details of alcohol and drug use, medical and psychiatric histories of self and relatives. The clinical data were obtained using the Bard/Porjesz adult alcoholism battery, a semi-structured clinical assessment schedule based on DSM IV criteria for the evaluation of clinical details of alcohol dependence and alcohol-related medical problems. Subjects classified as alcoholic were not analyzed in this study. Subjects were requested to abstain from alcohol and other central nervous system acting substances for 5 days prior to testing. Exclusion criteria included major medical conditions or current requirement of medication that could affect the central nervous system. Informed consent was obtained from each individual and they were paid for their services. Breath-analyzer tests were administered prior to recordings, and individuals with nonzero readings were excluded. Experimental procedures were approved by the Institutional Review Board and all subjects gave written informed consent.

2.2. Data collection

The subject was seated comfortably in a dimly lit, temperature regulated, sound attenuated (Industrial Acoustics Corp., Bronx, NY) room. Each subject was fitted with an electrode cap (Electro-Cap Intl. Inc., Eaton, OH) containing 61 electrodes. The nose served as the reference and the forehead as ground. Both vertical and horizontal eye movements were monitored. EEG activity was amplified 10 K (Sensorium, Charlotte, VT; bandpass: 0.02–50 Hz). The data were collected at a sampling rate of 256 samples per second for approximately 12.5 min and digitized by a Concurrent 5550 computer. Blinks were removed automatically offline by a spatial filtering method, and uncorrectable trials were removed from further analyses. The data were transformed to bipolar form by subtractions in software to produce 52 pairs of channels oriented vertically. Bipolar derivations were used to reduce volume conduction effects, and thus effect some degree of source localization, in preference to surface Laplacians because of the frequency domain effect of the Laplace transform (Le et al., 1994; Nunez et al., 1997). The data were resampled in order to have an integral number (32) of sample points per 120 ms cycle of background stimulus presentation. That is, every 32nd point in the resampled data corresponds to exactly the same state of background stimulus presentation. (This exact relation was made possible because the data acquisition system was driven by the video signal of the stimulus presentation system.) As a result of the resampling, algorithms for characterizing the relation between the observed oscillation and the photic driving stimulus are easy to implement. In addition, this enables any of the 120 ms time segments to be compared with any other, so that analytic methods characterizing a single stimulus cycle can be applied across all time segments taken as a group.

2.3. Data selection: examination of response to photic driving

Amplitude values for all subjects for a range of frequencies from 4 to 56 were obtained by the continuous wavelet transform, as described in the subsequent section (Section 3.2). (As a point of terminology, we call the activity in a given frequency band an *oscillation*; the time series obtained by an analytic method a *signal*.) In order to determine in which gamma frequencies, if any, periodic amplitude modulation at the photic driving frequency occurred, the *Z*-scores of the amplitude were calculated over all time points of the amplitude in each frequency band for each channel, and were then averaged across every 32nd point. Frequency bands from 29 to 43 Hz had a pronounced sinusoidal shape and ranged over an interval of at least 1.5 standard deviations. The peak of amplitude modulation was at 33 Hz; amplitude modulation declined gradually in frequencies above 48 Hz. The response curves of all frequencies of significance were quite similar. On the basis of these results, it was decided to examine the 33 Hz data in detail. The level of amplitude modulation was most pronounced in the occipital bipolar pairs (P3–PO7, P1–PO1, PZ–POZ, P2–PO2, P4–PO8, PO1–O1, POZ–OZ, PO2–O2), so only those channels were subject to analysis. The resultant data set had 336 subject–channel pairs (Fig. 1).

The first four figures illustrate the occurrence of gamma amplitude modulation in the grand mean of 42 subjects. The ripple pattern in the upper ranges of the first figure is *prima facie* evidence of gamma amplitude modulation. The amplitude modulation is apparent in Fig. 2, in which the entrainment of the alpha signal and the gamma amplitude modulation contrasts with the lack of entrainment of the gamma signal; compare the segments of the alpha signal which ascend from 0 to their maximum, with the adjacent ascending segments of the gamma

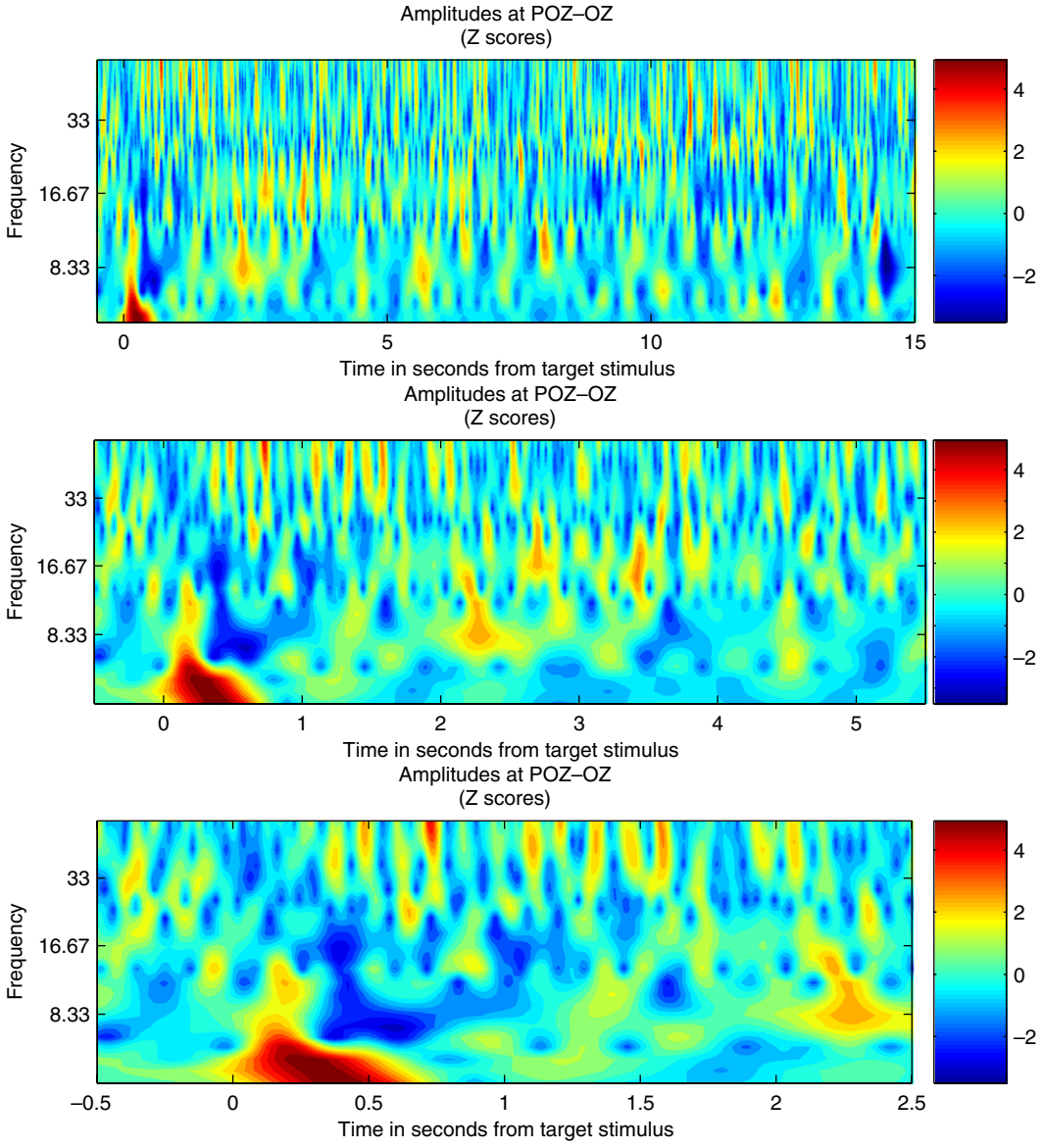

Fig. 1. Time–frequency amplitude plots at different time scales. Grand mean of time-locked CWT data from 42 subjects. *Z*-scores provide detail at higher frequencies otherwise unobtainable.

signal, which are far less regular. The average of every 32nd point in Fig. 3 shows the pattern of gamma amplitude modulation at the precise frequency of the photic driving stimulus; the alpha signal is shown below for comparison. It can be seen that the peak of the gamma amplitude trails the peak of the alpha signal by at least 30 ms. In Fig. 4, the multi-

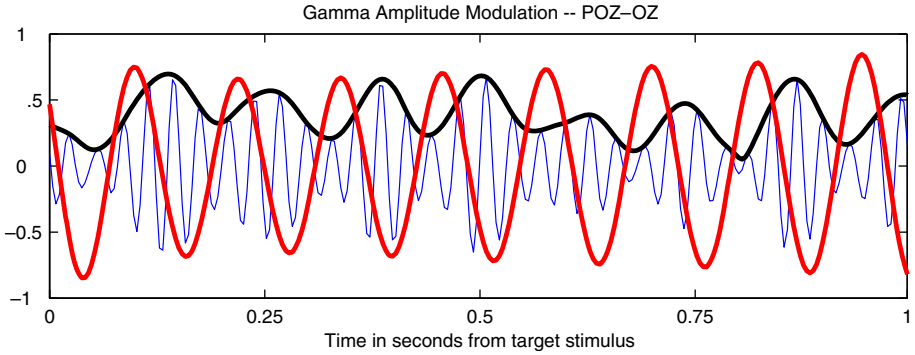

Fig. 2. Alpha signal (red) and gamma signal (blue); gamma amplitude (black) shows clear amplitude modulation with phase offset from alpha signal. Grand mean of time-locked CWT data from 42 subjects.

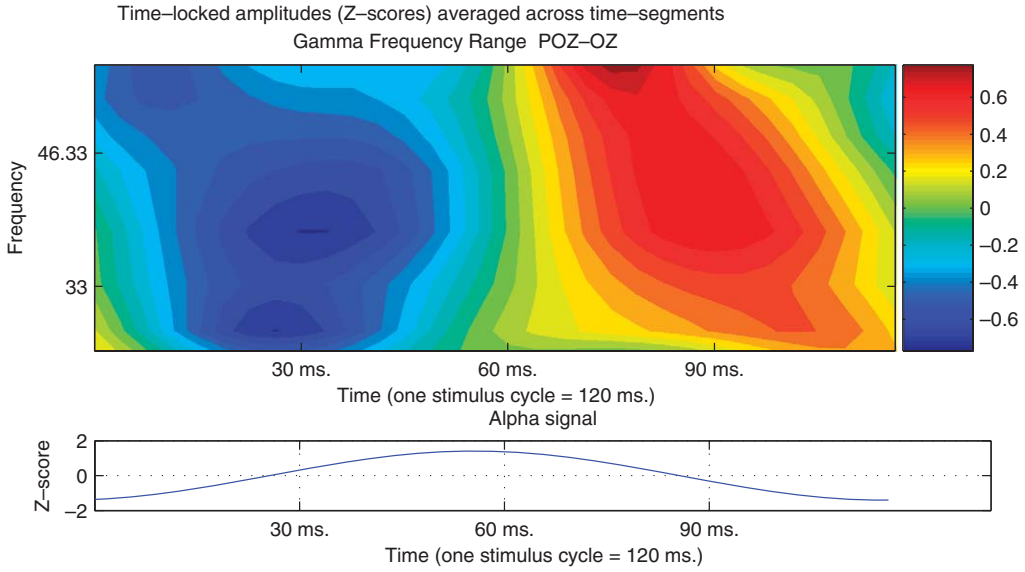

Fig. 3. Cross-segment averages in gamma amplitude show phase offset from the alpha signal.

taper estimate of the power spectrum reveals that there is some modulation at the harmonic as well.

3. Analytic methods

Our methods are designed to characterize both amplitude and frequency modulation in the recorded data, as both are significant in describing the behavior of oscillatory systems. There are two stages in our analytical process. In the first part time–frequency information from the recorded data is extracted using a continuous complex wavelet transform (Section 3.2); in the second the resulting information is analyzed to obtain both local and global characteristics of the oscillatory activity in the measured data. Time–frequency analysis, because it isolates the different frequency bands, providing information on their amplitude and phase, is the method appropriate to the oscillatory model. The result of the time–frequency analysis is a complex-valued time series for each frequency band analyzed for each trial. In the second stage our primary interests are the phase and amplitude relations between the signals under consideration. A number of phase clustering measures are applied to the complex values obtained by use of the continuous wavelet transform from the first stage of our analysis. The question of whether the gamma amplitude modulation (GAM) apparent from the first stage of analysis can be interpreted as a mathematical artifact of the methods of analysis is also considered; e.g. whether GAM could be simply the effect of a non-sinusoidal periodicity in the alpha signal or an effect of averaging. The second stage of our data analysis has three parts: First, the global character of gamma amplitude modulation is established by a power spectral analysis of the entire time series of gamma amplitude values (Section 3.3.2). Second, the phase relation of the gamma amplitude signal to the alpha signal in each cycle of the photic driving stimulus is determined, and its consistency over time is examined. Two methods are used to determine the phase relation in each cycle. One method consists of fitting time segments of the gamma amplitude signal to a sinusoid whose phase is a function of the phase of the corresponding alpha signal (Section 3.3.3). The other is an adaptation of

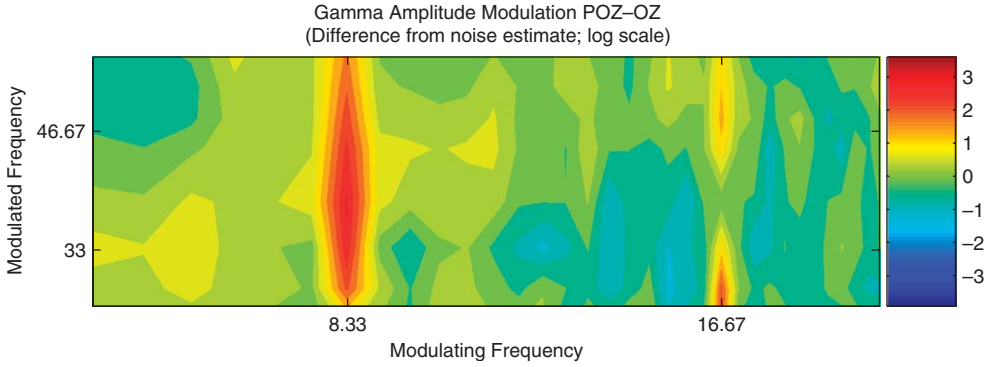

Fig. 4. Power spectral estimate of amplitude modulation in the frequency range 28–50 Hz. Each horizontal cross-section is the power spectrum minus the $1/f$ noise estimate of the signal whose center frequency is indicated on the y-axis. The pronounced peak at the alpha frequency is pervasive across the entire gamma frequency band. (See Section 3.3.2 for details on how these values were obtained.)

bispectral analysis to obtain phase relations between a modulated signal and a modulating signal (Section 3.4). A phase clustering index is used to measure the consistency of phase relations across time segments in each of these methods. Third, an intersegment phase consistency measure is used to examine single cycle gamma signals for the relation between frequency modulation and amplitude modulation by comparing points at the same time relative to the photic driving stimulus across different time segments (Section 3.5). This provides further information about the mechanisms producing GAM.

As we shall describe subsequently (Section 3.2), time series consisting of 4096 values were selected for analysis. In the power spectral analysis, the 4096 points of each time series under consideration are treated as a single sequence. In the sinusoidal fitting and bicoherence methods, they should be imagined as arranged in a 2-dimensional array with 128 rows of 32 points each. Each row is a 120 ms time series; each column corresponds to identical time in the background stimulus presentation. These methods operate on each of the 120 ms time segments, and then on the values obtained for each of the 128 segments. The intersegment phase consistency measure operates on each column of the array; then the resulting 32 point time series is considered.

3.1. Mechanisms of amplitude modulation

Amplitude modulation in an averaged signal can be the result of one or both of the following factors: First, amplitude modulation in the single intervals which make up the average; in this case the amplitude modulation must be consistent across intervals. Second, systematic frequency modulation in single intervals which result in the variation across time (in the averaged time series) of the phase consistency (phase-locking) across the trials which make up the average. (This is called phase resetting if the frequency modulation is relatively rapid.) Even if there were no amplitude modulation in the individual intervals, i.e. a constant amplitude in a segment, periods in a part of a time segment in which the intersegment phase consistency was greater than average would have greater cross-segment averages than periods in which the intertrial phase consistency was less than average. Thus amplitude modulation in the averaged signal can arise from variations in phase consistency across intervals; this is a real and neurophysiologically significant phenomenon which can only be revealed by the averaging process.

3.2. Time–frequency analysis: wavelet decomposition

In order to determine the precise temporal course of oscillatory activity in the sampled data, an analytic method which is capable of a high degree of temporal resolution is required, as well as a moderate width in the frequency domain. The continuous wavelet transform (CWT) method provides continuous output and the option of having multiple scales per octave. The complex Morlet wavelet was chosen for use because its sinusoidal shape approximates the shapes in the signal quite well. The use of a complex wavelet also enables phase relations to be examined directly (Lachaux et al., 2002; Rosenblum et al., 2004). In addition, this wavelet has been used in a number of other analyses (Herrmann et al., 1999; Krolak-Salmon et al., 2003), so its properties are familiar.

The resampling of the data enabled the choice of scales for the wavelet transform to match exactly the period of the entraining stimuli and its harmonics. For sake of completeness, the octave separated scales were supplemented with three additional scales for each octave, and placed as evenly as possible given the constraint of integer values for the scales. The scales ranged from 9 to 128 samples, providing a range from about 56 Hz to 4 Hz for the center frequencies of the Morlet wavelets. The complex wavelet transform, a convolution of the input signal with the complex Morlet wavelet

$$a^{-1/2} e^{\left(-(t/a)^2/2\right)} e^{2\pi i (t/a)}$$

where a is the scale, was used. (In our implementation of the CWT, a is the number of samples; the corresponding frequency is $(2*F)/a$, where F is the sampling rate; for the resampled signals $F=265.8$ samples/s.) The convolution of the complex Morlet wavelet with the single trial data results in a set of complex-valued time series for each subject. To produce the time series of non-time-locked values, the average over all trials of the amplitude of the elements of the complex time series is calculated. To produce the time series of time-locked values, the complex values are averaged across trials. Since there are periods of up to 30 s between successive target stimuli, meaningful cross-trial averages can be taken extending for up to 25 s succeeding the onset of each target stimulus. For the analysis, 15.4 s of averaged data, 4096 data points, extending from 1.6 s preceding the appearance of the target stimulus to 13.8 s subsequent to its appearance were used. These comprise 128 data segments, each of which contain one complete cycle of the periodic background stimulus. A preliminary examination of succeeding part of the time series with the same measures as discussed below revealed no differences from the earlier part, so values from it were omitted from the analysis. The initial focus of the analysis was the time-locked averaged data, with subsequent analysis of the non-time-locked averaged data. The number of trials included in each average ranged from 15 to 20, so there is no reason to expect significant differences in the signal to noise ratio in different temporal parts of the data analyzed.

The instantaneous amplitude and phase for each scale is immediately available from the complex-valued time series for each scale of the wavelet for the time-locked data. The real part of this time series is the signal as filtered by the wavelet, i.e. a bandpass filtered signal. The absolute value of the time series is the instantaneous amplitude of the bandpass filtered signal. When graphed, the instantaneous amplitude along with its negative looks like an envelope around the bandpass filtered signal; thus it is often called the amplitude envelope. The argument of the time series (inverse tangent of the imaginary part divided by the real part) is the instantaneous phase of the bandpass filtered signal. Amplitude modulation occurs when

the instantaneous amplitude has significant temporal structure; in this experiment the amplitude modulation of the alpha signal is related to the appearance of the target and non-target foreground stimuli and is aperiodic, while the amplitude modulation of the gamma signal is periodic, but is also affected by the appearance of the target stimulus.

3.3. Determination of gamma amplitude modulation

3.3.1. Methods of amplitude modulation determination

Several methods are employed to describe the characteristics of the periodic amplitude modulation and its relation to other features of the signals involved. The first is the simplest method of analysis, the calculation of the power spectrum of the gamma amplitude time series. This only determines whether amplitude modulation is present, but not the phase relation to the alpha signal. In order to characterize the phase relation of the gamma amplitude modulation to the alpha signal two additional methods are used. Segments of the gamma amplitude time series are fit to sinusoids whose phases are derived from those of the corresponding segments of the alpha signal. This is possible because of the integral length segments which contain exactly one period of the photic driving stimulus, and because both the alpha time series and gamma amplitude time series are roughly sinusoidal. A bispectral coherence method (bicoherence) which characterizes the phase relation of the alpha time series and gamma amplitude time series in a time segment is also employed. These two methods provide measures for amplitude modulation as well.

Before continuing with this discussion, the question of whether positive findings of gamma amplitude modulation could be a result of our method of analysis, rather than reflecting a real neurophysiological phenomenon must be addressed. Since the gamma amplitude modulation is at the frequency of the alpha signal, could the gamma amplitude modulation be a mathematical artifact arising from the possible non-sinusoidality of the alpha signal? Because a Fourier analysis of a periodic but non-sinusoidal signal decomposes the signal into a sum of sinusoids at the base frequency and higher harmonics of the base frequency, a wavelet analysis at the gamma frequency studied would capture one of the higher harmonics of the alpha signal, if it were present. If the gamma *signal* were an artifact of alpha harmonics, there would be a pervasive correlation between the gamma amplitude and the alpha amplitude. But statistical examination shows that there is no such correlation. When a regression of the mean gamma amplitude on the mean alpha amplitude in each segment is calculated over all the 128 segments of the entire time period studied, 335 of the 336 subject–channel pairs have an R^2 less than 0.2. This result is consistent with that obtained by Müller et al. (1997). But even if the amplitude of the gamma signal were correlated with the alpha amplitude, since the harmonics of a lower frequency signal produce sinusoids with *constant* rather than time-varying amplitudes, the observed amplitude modulation could not be the effect of alpha signal harmonic.

3.3.2. Spectral analysis of gamma amplitude

The power spectrum of amplitude of the gamma signal was calculated by the multi-taper method (Thomson, 1982) applied to all 4096 points for each channel of each subject. In addition to the estimated value for the power spectrum, one-tailed confidence limits for a number of confidence levels were also calculated. The estimated values and associated confidence limits were then log transformed since inspection of the spectra indicated that a major feature was $1/f$ noise. An appropriate metric distinguishes real amplitude modulation from noise in this situation. An estimate of the value of the power spectrum at the driving frequency due to random noise was calculated by linear interpolation using the estimated values at the frequencies distinct from the driving frequency and its harmonics. We fix the metric as the difference between the lower confidence limit for a particular confidence level for the calculated estimate at the driving frequency and the estimate of the value which would be expected from random noise. It will be called the spectral value for that confidence level. That is,

$$SpectralValue(\omega_0, a) = LowerConfLimitPS(\omega_0, a) - NoiseEstPS(\omega_0)$$

where a is the confidence limit, and $LowerConfLimitPS(\omega_0,a)$ is the lower confidence limit of the multi-taper estimate for frequency ω_0. In our case ω_0 is 8 1/3 Hz, the frequency of photic driving.

If the spectral value is non-negative, then the probability that the actual value of the power spectrum at that frequency is less than the noise estimate is equal to or less than the confidence level associated with that spectral value. The spectral values are to some extent independent of the estimate of the power spectrum at the driving frequency, and to a much greater extent of the absolute power of the gamma amplitude signal itself (see Figs. 5 and 6), and thus they are a better measure of the presence of amplitude modulation than the calculated estimate at the driving frequency.

3.3.3. Sinusoidal fitting of gamma amplitude

Given the periodicity of the gamma amplitude time series, the next step is to determine the relation between the phase of the gamma amplitude and the phase of alpha signal in short time intervals. In gamma amplitude signals with significant periodicity at the alpha driving frequency there should be a consistent phase difference between the gamma amplitude and alpha signal time series in a large number of time segments. It would be possible to measure the phase difference between the gamma amplitude and alpha signal time series by simply convolving each with the sinusoid $e^{2\pi i\omega_0}$ (ω_0=8 1/3 Hz) on each 32 point time segment, which is the Fourier method, and subtracting the phases. This procedure would be appropriate given the sinusoidal character of both the alpha signal and gamma amplitude modulation curves. However, it would not account for the relation between the frequency modulations in the alpha signal and gamma amplitude modulation curves. Therefore a method which made a direct match between the

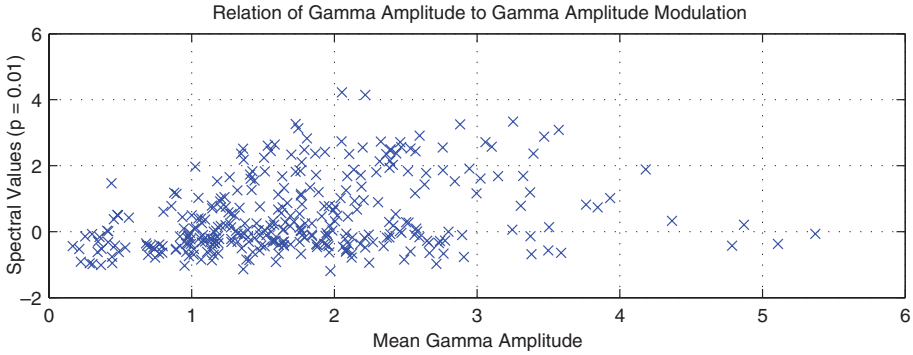

Fig. 5. Spectral value vs. gamma amplitude. Scatterplot of 336 subject–channel pairs. Everything below the line $y=0$ can be regarded as indistinguishable from noise.

phase values in the two curves was employed. A curve of the form

$$g(t) = a\cos(f(t) + b) + c\cos(2f(t) + d) + e$$

is fit to the gamma amplitude values in each segment, where $f(t)$ is the phase of the alpha signal at time t, by a least squares fit. The use of the phase of the alpha signal is an attempt to account for the inevitable but slight variations in the alpha signal within and between different segments. To model the slight degree of amplitude modulation at the harmonic, apparent in Fig. 4, a second cosine term is included. Goodness of the fit is measured by the ratio of the norm of the residual, which is the calculated value minus the data, to the norm of the data itself. Assuming that the form of the amplitude modulation is well represented by the sinusoid, and neglecting the harmonic term, the magnitude of the gamma amplitude modulation is given by a, the phase difference by b, and the mean of the gamma amplitude by e. If b is close to zero, the peaks of the gamma amplitude are aligned with the peaks of the alpha signal, while if b is close to π or $-\pi$, the peaks of the gamma amplitude are aligned with the troughs of the alpha signal. The a and b values can be represented by the complex value ae^{ib}, and a time series of these values, one value per segment, can be obtained. If the values are $u[t]$, then the phase clustering index (PCI) (Kalitzin et al., 2004), which is a weighted version of the synchronization index (Rosenblum et al., 2004) or phase-locking index (Klimesch et al., 2004)

$$\mathrm{PCI}(u[t]) = |\sum u[t]| / \sum |u[t]|$$

is a measure of the consistency of the alignment of gamma amplitude and alpha signal across segments (Miranda de Sa and Catelli Infantosi, 2002; Hurtado et al., 2004; van Milligen et al., 1995, 1997). It has a value ranging between 0 and 1. It is closely related to the coherence value which measures the phase consistency of a pair of signals. A weighted measure is preferred because low intensity noise will artificially lower an unweighted measure. By applying the PCI to the set of complex values obtained from the sinusoidal fitting process, one from each time segment, we obtain the sinusoidal phase index (SPI); it is a measure of the degree of gamma amplitude modulation, in that it measures how consistently the gamma amplitude signal mimics the shape of the alpha signal. If the value is high, then the argument of the mean of $u[t]$ represents the angular or phase difference between the alpha signal and the gamma amplitude signal, which can be converted to a time difference between identical features.

3.4. Bispectral analysis and bicoherence

A second method of determining the phase relation between the alpha signal and the gamma amplitude signal is to use bispectral analysis, in which the phase relations of three signals are used (Jamsek et al., 2003). Bispectral analysis and the bicoherence measure has generally been explicated in the context of the statistical analysis of higher order cross and autocorrelations (Schack et al., 2001, 2002; Schanze and Eckhorn, 1997), but an approach in terms of amplitude modulation seems appropriate in this context.

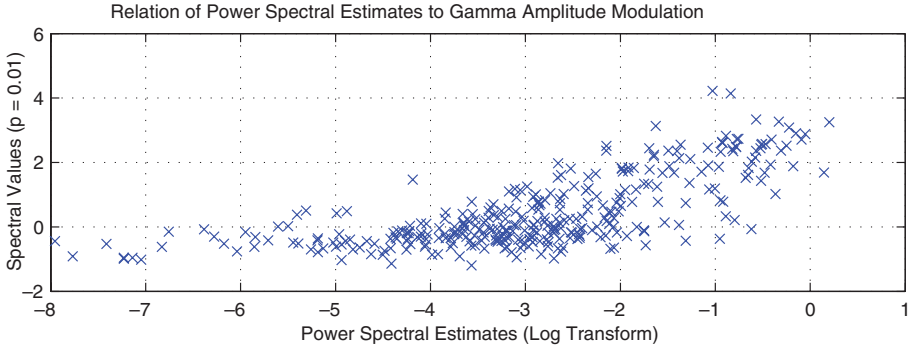

Fig. 6. Spectral value vs. power spectral estimate at 8 1/3 Hz. Scatterplot of 336 subject–channel pairs. Everything below the line $y=0$ can be regarded as indistinguishable from noise.

The familiar trigonometric identity

$$\cos(a)\cos\ (b) = (\cos(a+b) + \cos(a-b))/2$$

in the form

$$\cos(at+\phi_a)\cos(bt+\phi_b) = \big(\cos\big((a+b)t+\phi_{a+b}\big) + \cos((a-b)t+\phi_{a-b})\big)/2$$

where

$$\phi_{a+b} = \phi_a + \phi_b;\ \ \phi_{a-b} = \phi_a - \phi_b$$

suggests that in an amplitude modulated signal, where the modulation is sinusoidal, phase relations between signals at frequencies a, b, and either $a+b$ or $a-b$ should be consistent across time, that is, independent of t. Call the quantity $\phi = \phi_a + \phi_b - \phi_{a+b}$, or $\phi = \phi_a - \phi_b - \phi_{a-b}$, depending on the signals used, the phase resultant. It might be thought that this phase resultant would be zero, but as Jamsek et al. (2003) point out, the effect of the modulating signal on the modulated signal may be delayed, leading to a nonzero value. It is exactly this delay which is to be measured, since it corresponds to the phase difference revealed by the sinusoidal fitting method described in the previous section. In this context a would be the modulating frequency, in this case alpha; b would be the modulated frequency, in this case gamma; and $a+b$ or $a-b$ would be the frequency of the resultant signal, which would lie near that of the gamma signal. The phase resultant can be calculated for a time segment by adapting the phase clustering index to the case of 3 signals. The adaptation of phase clustering index used above, which will be called the bispectral clustering index (BCI), is obtained as

$$\mathrm{BCI}(u[t],v[t],w[t]) = |\sum\left(u[t]v[t]\widetilde{w[t]}\right)|/(\sum|u[t]|\sum|v[t]|\sum|w[t]|)$$

or

$$\mathrm{BCI}(u[t],v[t],w[t]) = |\sum\left(u[t]\widetilde{v[t]}\widetilde{w[t]}\right)|/(\sum|u[t]|\sum|v[t]|\sum|w[t]|)$$

over each time segment, where $u[t]$ is the complex representation of the alpha signal, $v[t]$ is the complex representation of the gamma signal and $w[t]$ is the complex representation of the signal whose frequency is the sum or the difference of the alpha and gamma frequencies, all derived from the CWT. The conjugation of the gamma signal depends on whether the frequency of the third signal is the sum or difference of the frequencies of the first two. Angular differences, computed by taking the arguments of complex values appearing in the numerator of the preceding equations, reflect the relative phase relations of the modulated and modulating signals, and are meaningful if the BPI is high. The BPI for a single time segment is expected to be high because of the band-limited nature and non-independence of the summands in a single 32 point time segment. Taking the complex values from this operation, that is, omitting the absolute value operation in the numerator, a set of values is obtained whose PCI indicates the phase consistency of amplitude modulation over the entire time course of the 15 s duration of the averaged signal. We call the PCI applied to these values the bispectral phase clustering index (BPCI).

3.5. Intersegment phase consistency

As we have mentioned, one of the factors that could produce amplitude modulation in the time-locked signal is frequency modulation in the single trials, or phase resetting. Phase resetting occurs when the distribution of phases (across time segments) at any one time in the alpha cycle differs (by becoming more or less concentrated) from the distribution at an earlier time. It is measured by the same phase clustering index we have used previously. Consistent variation in the PCI across the 32 points in a cycle indicates the presence of frequency modulation, which is the characterization of the change in phase progression in a single signal which must occur in some trials for there to be phase resetting. In order to confirm the consistency of the phase relations between different segments of the gamma amplitude time series and test the degree to which the amplitude modulation is caused by frequency modulation, the PCI of the gamma signal at equivalent times relative to the photic driving stimulus was calculated. That is, every 32nd point of the complex-valued times series for the gamma signal is taken, in our case 128 points, and the PCI, as defined in the preceding section, is computed. For each subject–channel pair 32 values are obtained, showing the phase consistency over time at each distinct moment of the photic driving stimulus. (For a discussion of phase resetting in the context of evoked potentials, with informative illustrations, see Klimesch et al., 2004, esp. p. 303.)

4. Results

4.1. General pattern of alpha and gamma activity

Before discussing the 33 Hz amplitude modulation, a brief account of the occipital alpha activity is in order. The alpha signal was pronouncedly sinusoidal, in accordance with the pattern reported by Regan (1989), even though the photic driving stimulus is not sinusoidal but a square wave. The alpha band activity at the driving frequency has a post-target increase above pre-target levels persisting to 300 ms post-stimulus-onset, then decreasing to about 1000 ms post-stimulus-onset, followed by recovery, as is apparent in Fig. 1. The change between the immediate post-target maximum and the following minimum is greater than 5 standard deviations in the signal taken over a 5 s period. A similar but less intense pattern follows the change from the target to the non-target foreground stimulus. Our previous paper has a more thorough discussion (Chorlian et al., 2003).

Turning to the gamma amplitude modulation, Fig. 5 shows that gamma amplitude modulation is not highly correlated with the overall level of gamma activity; while Fig. 6 shows that there is a threshold level of random fluctuation in gamma amplitude below which no significant gamma amplitude modulation takes place. Fig. 7 shows that power spectral estimates of gamma amplitude modulation correlate strongly with those derived from phase clustering indices. The Fisher Z-transform (inverse hyperbolic tangent) was applied to PCI data

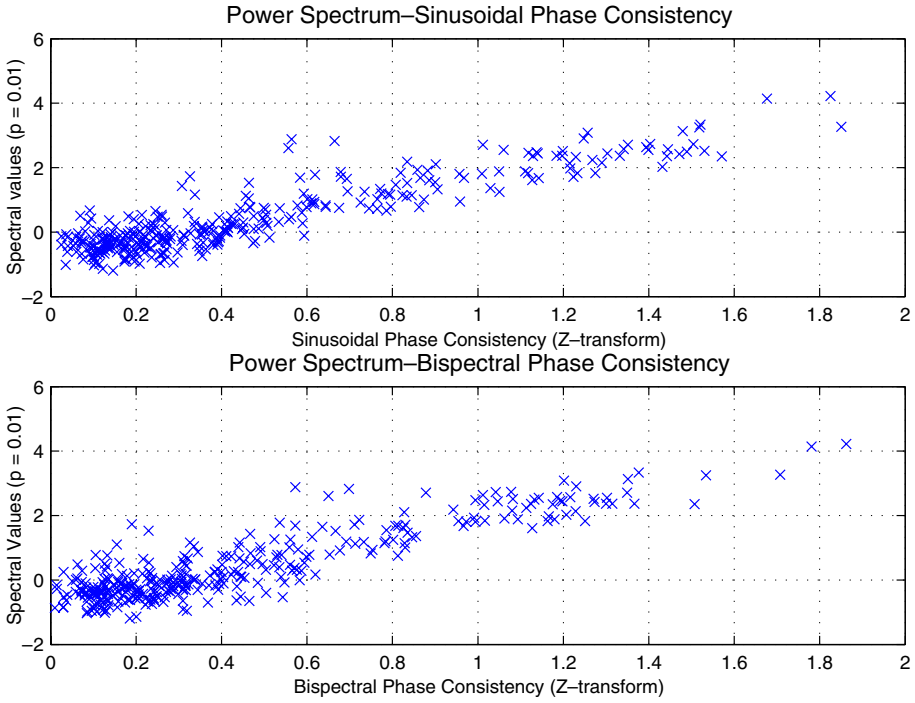

Fig. 7. Spectral value vs. two estimates of phase consistency. Scatterplot of 336 subject–channel pairs.

in order to spread out values at the top of the scale (Bendat and Piersol, 1971).

4.2. Power spectrum of gamma amplitude

Of the 336 subject–channel pairs, 226 (67%) had significant gamma amplitude modulation determined at the $p=0.05$ level, and 178 (53%) at the $p=0.01$ level. Central channels (PZ–POZ, POZ–OZ) had more subjects with significant values than peripheral channels (Table 1).

4.3. Sinusoidal fitting of gamma amplitude

The phase clustering index was calculated for those time segments in which the norm of the residual was less than 25% of the norm of the data. In general, the value was correlated with the number of segments used to calculate it ($R^2=0.5853$). In those subject–channel pairs in which the phase clustering was greater than 0.5 there is a strong statistical connection between the sinusoidal phase clustering values and the spectral values (a regression of the two values gives $R^2=0.8202$). The fact that many more subject–channel pairs had significant gamma amplitude modulation at the $p=0.01$ level than had an SPI greater than 0.5 suggests than gamma amplitude modulation often does not occur consistently across the entire extent of the 15 s time interval studied (Fig. 8, Table 2).

4.4. Phase clustering

The mean phase differences between the alpha signal and the GAM signal in those subject–channel pairs with high phase clustering were remarkably consistent. The value for the phase difference ('*b*' in the equation in Section 3.3.3) was concentrated between −90° and −180°, corresponding to a 30 ms–60 ms time difference, with the gamma peak trailing the alpha peak for all subject–channel pairs which had significant gamma amplitude modulation. As the between segment phase clustering increased, the phase differences of subject–channel pairs were grouped more closely. This seems to be conclusive evidence that the phase difference between alpha signal and gamma amplitude measures a distinct neurophysiological variable. In the bispectral phase clustering method, the sum of the phases of the modulated and modulating signal is not equal to the phase of the resultant signal. That is, the peak of the gamma amplitude signal, the resultant signal, does not coincide with the peak of the alpha signal, the modulating signal, because the amplitude modulation is mediated by some neural system and is not a purely mathematical effect, as noted in Section 3.4. The bispectral phase clustering index estimates have the same character as the sinusoidal phase clustering estimates. There is a strong agreement between the angular values representing the time delay between the alpha signal and the gamma amplitude obtained from the sinusoidal fit and those

Table 1
Prevalence of gamma amplitude modulation by channel

Channels	P3–PO7	P1–PO1	PZ–POZ	P2–PO2	P4–PO8	PO1–O1	POZ–OZ	PO2–O2	Total (out of 336)
N subs, $p=0.01$	18	24	26	24	20	19	25	22	178 (53%)
N subs, $p=0.05$	28	29	35	28	25	23	32	26	226 (67%)

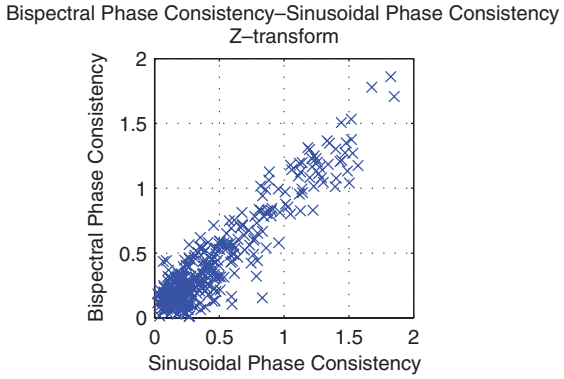

Fig. 8. Bispectral phase clustering vs. sinusoidal phase clustering. Scatterplot of 336 subject–channel pairs.

obtained from the bispectral method. The difference between the corresponding angular values had a mean of less than 5° and a phase clustering index of at least 0.9670 when measured across subject–channel pairs with significant amplitude modulation. The difference can be accounted for by the presence of extraneous components in the resultant frequency signal. Table 3 provides the PCI of the mean phase values from the subject–channel selection indicated in the top row of the table (Fig. 9).

4.5. Relations of phase consistency and amplitude modulation measures

Regressions showing the relation between the various measures of gamma amplitude modulation use all 336 subject–channel values. Measures are as described above. There is a strong statistical connection between the bispectral phase clustering and both the spectral values and the sinusoidal phase clustering values. The R^2 for the regression of spectral values on the bispectral phase clustering was 0.7978, and for the regression of the sinusoidal phase clustering R^2 was 0.8099 (Table 4).

4.6. Intersegment phase consistency

The graph of the intersegment phase clustering indices, described in Section 3.5, averaged over all subjects shows a marked quasi-sinusoidal shape for each channel, which means that there is a regular cycle of drift from uniformity of phase across time segments to a state where phase is less uniform across segments followed by the opposite process, demonstrating frequency modulation or phase resetting. Selecting those subject–channel pairs which show the most gamma amplitude modulation, the cycle becomes more pronounced, as a result of an increase in the maximum value of the phase clustering index. This is confirmed by examination of the coefficient of variation (standard deviation divided by mean) of the gamma amplitude curves taken across time segments. It was greatest at the minimum of amplitude modulation and least at the maximum. When the time segments of the non-time-locked gamma signal is similarly averaged across corresponding time points, a similar quasi-sinusoidal shape is found. The graph of the non-time-locked gamma shows "pure" amplitude modulation, that is, unaffected by frequency modulation. The value of the maximum of the intersegment PCI and the difference between the maximum and minimum values of the non-time-locked amplitude are most correlated with the spectral value; neither the difference between the minimum and maximum value of the intersegment PCI, nor the value of the maximum of the non-time-locked amplitude have a high degree of correlation with the spectral value. The R^2 for the regression of the spectral values on the pair maximum of the intersegment PCI and the proportional difference between the maximum and minimum values of the non-time-locked amplitude was 0.8948, with the values for the single variables 0.7996 and 0.6088 (Fig. 10).

Table 3
Phase clustering measures across subject–channel pairs

Subject–channel selection	SPI>0.5	SPI>0.6	SPI>0.7	SPI>0.8
Sinusoidal phases	0.6549	0.7044	0.7632	0.8038
Bispectral phases (sum)	0.7278	0.7952	0.8226	0.8620
Bispectral phases (difference)	0.5699	0.6021	0.7029	0.7535
Sinusoidal-bispectral (sum)	0.9670	0.9681	0.9695	0.9763
Mean angular difference (radians)	0.0915	0.0959	0.0966	0.0859
Sinusoidal-bispectral (difference)	0.9242	0.9368	0.9306	0.9562
Mean angular difference (radians)	−0.0748	−0.1122	−0.1191	−0.0892

4.7. Alpha–gamma amplitude relation

There is an inverse correlation between the levels of the gamma amplitude and the levels of the alpha amplitude during the period extending from the target stimulus to about 750 ms subsequent to the stimulus. The result was established in the following manner: First, gamma amplitude values were smoothed by a 32 point boxcar filter, corresponding to the length of one alpha cycle. Then, all alpha and gamma amplitude values extending over the 15 s period of analysis for each of the 336 subject–channel pairs were transformed to Z-scores on a per channel basis. The times of the maxima of the alpha amplitudes during the 0–750 ms post-target interval were determined, and then the times of the minima of the alpha amplitudes subsequent to the alpha amplitude peak, and the

Table 2
Prevalence of gamma amplitude measured by sinusoidal phase index (SPI)

Channels	P3–PO7	P1–PO1	PZ–POZ	P2–PO2	P4–PO8	PO1–O1	POZ–OZ	PO2–O2	Total (out of 336)
SPI>0.9	0	1	2	0	0	3	2	2	10
SPI>0.8	3	7	8	4	2	8	5	5	42
SPI>0.7	4	8	10	5	5	8	9	8	57
SPI>0.6	7	13	17	8	6	9	10	9	79
SPI>0.5	10	15	20	13	9	12	13	11	103

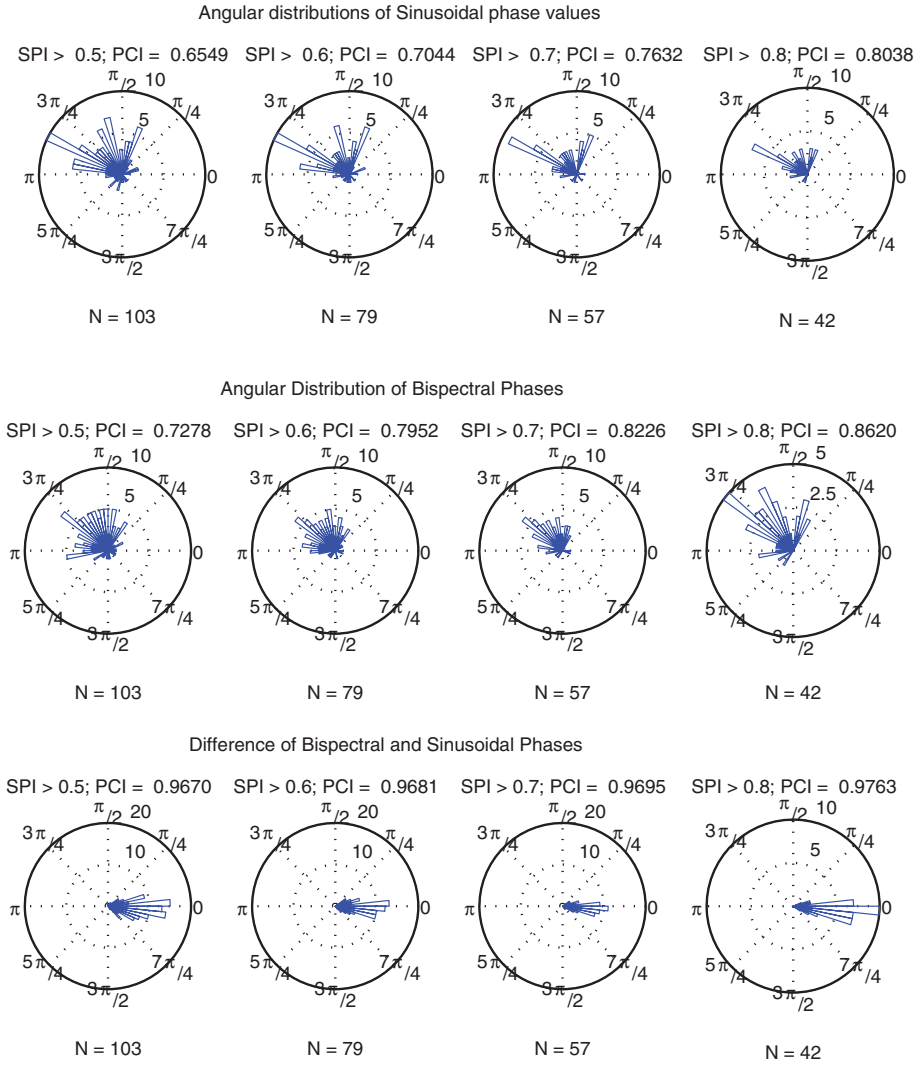

Fig. 9. Phase distributions derived from sinusoidal and bispectral analyses. The third panel shows the distribution of the difference between phases derived by the two methods for the same subject–channel pairs. '*N*' designates the number of subject–channel pairs in the histogram.

means of each of the gamma amplitudes taken over a 60 ms period centered at each of those times were calculated. Then the gamma value at the later time was subtracted from the value at the earlier time. If there were no relation between the gamma amplitude and the alpha amplitude one might expect the values for the sign of the gamma subtraction to be random. Instead, 210 of the 336 (62.5%) subject–channel pairs had negative signs; if positive and negative signs for gamma were equally likely, the probability of getting at least as many negative signs for gamma as the observed result is 0.000003. The corresponding percentage was 76% for those with significant gamma amplitude modulation. The distribution of gamma subtraction values was compared to a normal distribution with mean 0 and standard deviation determined from the differences of gamma values selected in a similar manner from randomly chosen intervals; a Kolmogorov–Smirnov test showed that the two distributions were not identical.

Table 4
Consistency of phase indices measured by regression coefficients

	R^2	F	p
Spectral value-SPI	0.8202	1523.7086	0.0000
Spectral value-bicoherence (sum)	0.7978	1318.0575	0.0000
Spectral value-bicoherence (difference)	0.7788	1176.0228	0.0000
SPI-bicoherence (sum)	0.8041	1371.0698	0.0000
SPI-bicoherence (difference)	0.8099	1422.7265	0.0000

5. Summary

Gamma amplitude waveforms are maximally aligned across time segments 50 ms after a local maxima of the alpha signal; then they become less consistent across time segments over an interval of half an alpha period. At that point a phase resetting process begins, with a concomitant realignment of the amplitude waveforms. The phase of the alpha signal when the resetting occurs is quite consistent across individuals and channels, as well as across time within individuals. The precise phase of the gamma signal when the resetting occurs seems not to be consistent between individuals; but it does seem to be somewhat consistent over time and channels within individuals. In

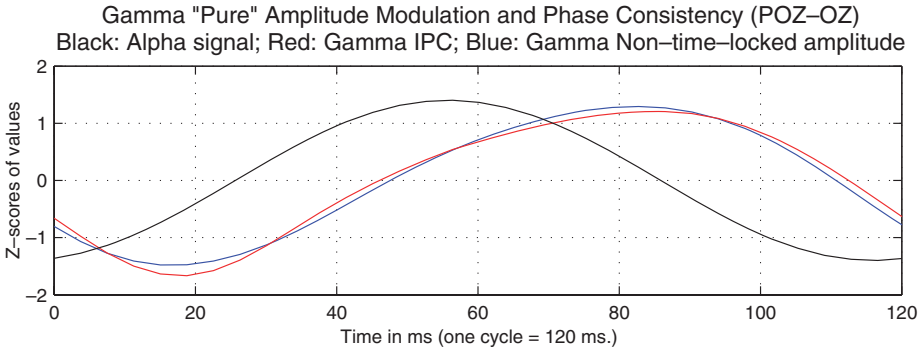

Fig. 10. Relation between alpha signal and sources of gamma amplitude modulation.

addition, examination of the non-time-locked gamma amplitude shows that there is simultaneous "pure" amplitude modulation. Frequency modulation, found in phase resetting, unlike "pure" amplitude modulation, requires a speeding up or slowing down of some neural process; amplitude modulation can occur simply by the recruitment of neural ensembles to an ongoing process. This indicates that process driving the GAM is of an intermittent quality, having its effect only during the period during which the intersegment phase consistency is increasing. In other words, photic driving produces time-locked gamma amplitude modulation, that is, entrainment of the gamma *amplitude* signal, both by single trial amplitude modulation and by phase resetting. The determination of the presence of gamma amplitude modulation and the angular or phase relations between signals was made through the use of several distinct algorithms, all of which gave similar results. The consistency of the results between these methods is striking. In addition, the presence of the inverse relation between alpha amplitude and gamma amplitude modulation in the 750 ms post-target-stimulus period is significant in determining the precise relation between the alpha and gamma oscillatory systems.

6. Discussion

The presence of gamma amplitude modulation at the frequency of the appearance of the background stimulation indicates that this particular form of gamma production has a definite sensory character. This, and the consistent phase relation between the alpha signal and the gamma amplitude modulation time series, leads us to consider why evoked sensory gamma oscillation might be susceptible to amplitude modulation. We note the following results from evoked potential experiments which produce early evoked sensory gamma, with the explicit caveat that the entrainment of the alpha oscillation by photic driving might produce different patterns of electrophysiological activity than those produced in evoked potential experiments.

6.1. Features of gamma production

(1) Gamma production is immediate post-stimulus onset, with gamma first appearing within 50–100 ms.
(2) Gamma is often followed within 30–80 ms by alpha activity (Fell et al., 1997; Karakas et al., 2001; Karakas and Basar, 1998; Sannita et al., 2001; Sannita, 2000; Senkowski and Herrmann, 2002; Tomberg and Desmedt, 1998); it must be noted that this is often only apparent in the figures, and not in the authors' discussions.
(3) Gamma production is burst-like, with the duration of bursts lasting 50–150 ms. The duration, and in some cases the shape of the waveforms indicate amplitude modulation which falls in the alpha range (Carozzo et al., 2004). Whether the cessation of gamma production found in these cases is an intrinsic property of the gamma generating system or the result of interaction with other oscillatory systems is not determinable from the evidence presented. (Neural mechanisms for burst production are apparently more sensitive to low frequency stimulation (Oswald et al., 2004); some models of neural gamma production show low frequency bursting (Doiron et al., 2001; White et al., 2000).)
(4) Gamma exhibits resonance characteristics in some experiments. By resonance we mean that the system continues to produce output after the stimulus condition which elicited the initial output is no longer present. In a number of experiments eliciting gamma in humans there seem to be gamma bursts subsequent to the initial gamma burst (Herrmann et al., 1999; Senkowski and Herrmann, 2002; Bakhtazad et al., 2003). Only the initial burst is the response to the appearance of the stimulus while subsequent bursts occur while the stimulus is present. This is particularly significant considering Busch's demonstration that early evoked gamma is as much a response to a transition from one stimulus state to another as to the stimulus itself. In recordings from the rat visual cortex, Imas et al. (2004) found gamma resonance in unanesthetized and low dose anesthetized animals. We note that there seem to be resonance characteristics in other oscillatory systems; Di Russo et al. (2001, 2005) show resonance in alpha to a single pattern reversal. In steady-state visual evoked potentials produced by response to flicker, it is well known that alpha exhibits resonance (Regan, 1989). Parra et al. (2003) show what might be resonance to low frequency stimulation.

In a paper which describes a number of experiments which characterize the temporal response profiles of sensory gamma, Busch et al. (2004) clearly demonstrate the first and third

characteristics noted above. Since they do not analyze the low frequency components in the responses of the subjects, they provide no evidence regarding our second characteristic. Since the durations of the stimuli eliciting the gamma response are not long enough for the resonance effect to occur, they provide no evidence regarding our fourth characteristic. All of these characteristics of gamma are found in response to aperiodic stimuli; they suggest that the gamma system might be seen as governed by a damped resonator with a characteristic frequency ranging from 6 to 10 Hz, judging by the characteristic duration of a burst. Pursuing this analogy, we speculate that the photic driving at or near the resonant frequency will cause repeated bursts which are seen as periodic amplitude modulation. In addition, Stefanics et al. (2004) found that repeated instances of the same stimulus produced more early evoked gamma than did sequences of disparate stimuli. It is possible that the constant repetition of the background stimulus is particularly suited to stimulating the resonance properties of the gamma oscillatory system.

The evidence for direct interaction between gamma and lower frequency activity is more scattered. von Stein et al. (2000) report phase coupling between high and low frequencies between different areas in the visual system of cats in response to visual stimuli in the first 500 ms following stimulus presentation. Schanze and Eckhorn (1997) report phase coupling between high and low frequency activity in the visual cortex of the cat and the monkey, but this is not directly stimulus related. Some degree of gamma amplitude modulation has been found in cats: by Kayser and Konig (2004) in the 23–36 Hz range, and by Volgushev et al. (2004) in the visual cortex. Volgushev states, "... visual cortex neurons may use a kind of amplitude modulation of the high-frequency component to encode the temporal structure of the response in the low frequency range. The use of the amplitude modulation encoding may expand the borders of applicability of stochastic resonance to the function of nerve cells" (Volgushev et al., 2004, p. 961). Kruse and Eckhorn (1996) report what might be interpreted as inhibition of gamma by alpha in cats. Bruns and Eckhorn (2004) report what might be amplitude modulation in gamma in a human subdural recording. Parra et al. (2003) in an experiment with a somewhat similar photic driving stimulus, but otherwise quite different, report entrainment of gamma range oscillations during photic stimulation. Parra et al. speculate that, "These observations suggest that the enhancement of the gamma-band PCI in our experiments is possibly related to natural non-linear resonance properties of the visual system ... the enhancement of synchrony in the gamma band of photosensitive patients may reflect a loss of control of the brain over a high-frequency oscillatory process that normally operates to transiently connect neural assemblies involved in the cerebral cortex ..." (Parra et al., 2003, p. 1168). They do not discuss whether the controlling factors in their theory involve the alpha generating system. It is possible that some of the neural mechanisms mentioned by them are also involved in gamma amplitude modulation. (It should be made clear that the entrainment of gamma oscillations found by them is not the same phenomenon as the entrainment of gamma amplitudes reported here.)

6.2. Alpha–gamma interaction

On the basis of our own data and current evidence from the literature, we offer three hypotheses for a possible mechanism of the gamma amplitude modulation for consideration of which the third seems the most plausible:

(1) Alpha entrainment and gamma amplitude modulation are completely separate; each is the result of the photic driving. The amplitude modulation of gamma is produced by the alternation of ON and OFF stimuli. The gamma phase resetting and consequent increase in amplitude is produced by each ON stimulus. In this case, the duration of the OFF stimulus must be long enough to allow the gamma system to recover to the point of responding to the subsequent ON; but this seems inconsistent with Busch's finding that there is gamma to the OFF in evoked potential experiments. The alpha entrainment is produced in the same manner, but the relation of the wave shape to the ON and OFF phases of the stimulus is difficult to determine (Regan, 1989, pp. 382–384). Once the system which is responding to the photic driving starts, it has its own output dynamics. This hypothesis seems to be in accord with the speculation of Sewards and Sewards (1999) that gamma and alpha oscillations in the visual system are generated independently, but that the gamma oscillations are at precisely three times the frequency of the alpha oscillations. We do find the peak of gamma amplitude modulation to be three times the frequency of the driving stimulus, but we do not find alignment of the gamma signal with the alpha signal as these authors speculate. (It is not clear how such precise synchronization is to occur if the systems do not interact.) This hypothesis is unable to account for the post-target inverse relation between alpha and gamma amplitudes. In addition, it makes the consistency in the phase relation between the gamma amplitude modulation and the alpha signal purely coincidental.

(2) Alpha entrainment drives gamma amplitude modulation in a unidirectional manner. That is, alpha activity at a particular phase in its cycle causes the phase resetting in the gamma cycle. Thus in this case there is no clear relation between the stimulus and the gamma amplitude waveform, because there is no clear relation between the stimulus and the alpha waveform. This hypothesis is suggested by some network models (Doiron et al., 2001; White et al., 2000). It would also account for the consistency in the phase relation between the two systems. However, it is inconsistent with the post-target inverse relation between the amplitudes of the systems. It also seems inconsistent with evoked potential experiments, noted in Section 6.1, in which gamma precedes alpha on sensory stimulation. It should be noted that the situation in the steady-state case may be different from what occurs in an evoked potential experiment.

(3) Gamma and alpha are connected by a feedback mechanism in which gamma drives the alpha entrainment and is

then inhibited by the alpha, and restimulated by the ON stimulus. This would mean that amplitude modulation of gamma is a result of stimulus variation plus an intrinsic feedback loop in gamma–alpha circuitry. This is in accordance with the data from this experiment and the reported gamma in evoked potential experiments. In some of the evoked potential experiments the gamma is diminished after the occurrence of alpha on sensory stimulation (Senkowski and Herrmann, 2002); this would be consistent with the observed data, as there is no sensory input to restimulate gamma in these circumstances. It should also be noted that although the background photic driving stimulus is discontinuous, only the gamma signal evidences any form of periodic intermittency; the alpha signal shows no sign of phase resetting in response to the photic driving stimulus; only the presence of a new foreground stimulus produces any phase resetting in alpha (Chorlian et al., 2003). One explanation of this is that the alpha sinusoidality is mediated by the gamma system, which acts to smooth the alpha response. In addition, if we accept the finding by Busch et al. (2004) that the gamma amplitude response to a short duration stimulus is longer than that to a long duration stimulus because of the merger of the response to the ON and OFF patterns, the pattern of gamma amplitude modulation observed in this experiment could not be governed by the intrinsic duration pattern of the gamma system, if there were such a pattern. That is, following Busch, if we assume that 60 ms stimuli will have the same gamma generating properties as the 50 ms stimulus considered in that experiment, we would expect the heightened gamma activity to be at least 100 ms in duration, gathering from their Fig. 6B (Busch et al., 2004, p. 1816). Clearly something must be acting to prevent the extended gamma activity from occurring in our experiment. The obvious candidate is the similarly periodic alpha activity. Further, if we examine Busch's figure more closely, we observe that the gamma bursts are about 50–80 ms in duration, so one might fairly conclude that in our case the OFF response is completely suppressed. It is not only suppressed but *reversed*, in that the gamma amplitude curve has a pronounced sinusoidal shape, with equal periods of activation and deactivation. This is beyond the simple extinction of the gamma response. The hypothesis of gamma–alpha feedback also fits a pattern in which a higher frequency activity is followed by lower frequency activity and concurrent inhibition of the higher frequency by the lower frequency (von Stein and Sarnthein, 2000). This pattern is exemplified in the target trials in visual oddball evoked potential experiments: there is initial alpha at P1–N1, which is sensory-perceptual, followed by a theta–delta increase and alpha decrease at P3 (Klimesch et al., 2004; Gruber et al., 2005).

The particular sensory event to which the gamma is a response is the background flicker, as shown by the constancy over time of the response and its occipital focus. We hypothesize the following course of gamma activity: Gamma is evoked by the transition to the ON phase of the background stimulus (Volgushev et al., 2003). This appears as the beginning of the phase resetting of the gamma. Drawing on the evoked potential results we note the following: Gamma phase resetting is suggested in several papers as the explanation of the time-locking of gamma activity in the immediate post-stimulus period (Fell et al., 1997; Tomberg and Desmedt, 1998). As a result of the time-locked gamma activity, alpha activity is enhanced. In the evoked potential experiments in which early sensory gamma is reported, N1 activity, which is in the alpha band, immediately follows the gamma activity. An interpretation of P1–N1 activity is that it is caused by a post-stimulus phase resetting of alpha and/or theta (Makeig et al., 2002; Klimesch et al., 2004; Gruber et al., 2005). This phase resetting of alpha could be the result of gamma activity. The alpha activity then inhibits the gamma activity. There is some evidence of gamma being inhibited by alpha as noted above. And there is evidence of gamma affecting alpha. In fact, Bruns and Eckhorn (Bruns and Eckhorn, 2004, p. 113) state, "... [the gamma] process associated with the envelopes influenced the process associated with the low-frequency signals (and not vice versa). Starting from this assumption, we can speculate about the possible underlying neuronal mechanisms. In short, envelope-to-signal correlation may result from a transmission of temporally modulated gamma-activity via a pathway with temporal dispersion."

Characterizing the interaction of the gamma and alpha systems in an experiment which produces what is essentially a steady-state response on the basis of evoked potential findings is speculative. The decline in amplitude of early evoked gamma in the evoked potential experiments could either be from inhibition by alpha or other lower frequency activity, or of the lack of new sensory content, because of the short duration of the stimuli presented. Nevertheless, we would point to a report by Fell et al. (2002), which describes a situation in which impairment of attention is explained by the suppression of gamma activity by a lower frequency activity, and the consequent absence of the gamma activity resulting in a failure to activate a subsequent lower frequency process. Fell describes a situation which is completely in the evoked potential context, yet one might imagine a similar process, i.e. using similar neural pathways, as the explanation of our findings. In our experiment, the background photic driving continually restimulates the gamma, which is continually inhibited by the engendered alpha. This seems to be consistent with the network model offered by White: "...bursts at gamma frequencies with periodic interruptions every theta cycle," (White et al., 2000, p. 8129), as reflected in their plot of gamma and theta spiking in response to an 8 Hz continuous stimulus (White et al., 2000, Fig. 4, p. 8131). After the inhibition associated with the descending phase of the alpha signal, the gamma is then restimulated by the reappearance of the ON phase of the background stimulus. In producing the observed gamma amplitude modulation, frequency modulation and pure amplitude modulation in gamma occur roughly simultaneously; this suggests that the gamma system responds both qualitatively and quantitatively to the photic stimulus. The steady-

state response to photic driving involves an interaction between a number of neural assemblies, as is apparent from Fig. 1; only the interaction between alpha and gamma is considered here.

Acknowledgements

We would like to thank Nancy Kopell who read some early drafts; her questions contributed greatly to clarifying the intent of the paper. Our colleagues at the Neurodynamics Laboratory were extremely helpful; among them, Ajayan Padmanabhapillai provided useful comments regarding the gamma producing evoked potential experiments and Madhavi Rangaswamy asked searching questions about the relation of the functional interpretation to the actual observations. We would also like to thank a former colleague, Kongming Wang, for discussions regarding the mathematical analyses used herein. The comments of a number of anonymous reviewers contributed to a significant clarification of the exposition.

References

Azizi, S., Ogmen, H., Jansen, B.H., 1996. A unified analysis of alpha rhythm, fast synchronized oscillations, and flash visual evoked potentials. Neural Netw. 9, 223–242.

Bakhtazad, L., Shumikhina, S., Molotchnikoff, S., 2003. Analysis of frequency components of cortical potentials evoked by progressive misalignment of Kanizsa squares. Int. J. Psychophysiol. 50, 189–203.

Basar, E., Basar-Eroglu, C., Karakas, S., Schurmann, M., 2001a. Gamma, alpha, delta, and theta oscillations govern cognitive processes. Int. J. Psychophysiol. 39, 241–248.

Bendat, J., Piersol, A., 1971. Random Data: Analysis and Measurement Procedures. Wiley-Interscience, New York.

Bruns, A., Eckhorn, R., 2004. Task-related coupling from high- to low-frequency signals among visual cortical areas in human subdural recordings. Int. J. Psychophysiol. 51, 97–117.

Burgess, A.P., Ali, L., 2002. Functional connectivity of gamma EEG activity is modulated at low frequency during conscious recollection. Int. J. Psychophysiol. 46, 91–100.

Busch, N.A., Debener, S., Kranczioch, C., Engel, A.K., Herrmann, C.S., 2004. Size matters: effects of stimulus size, duration, and eccentricity on the visual gamma band response. Clin. Neurophysiol. 115, 1810–1820.

Carozzo, S., De Carli, F., Beelke, M., Saturno, M., Garbarino, S., Martello, C., Sannita, W.G., 2004. Factor structure of the human gamma band oscillatory response to visual (contrast) stimulation. Clin. Neurophysiol. 115, 1669–1676.

Chorlian, D.B., Porjesz, B., Begleiter, H., 2003. Determination of human EEG alpha entrainment ERD/ERS using the continuous complex wavelet transform. Proc. SPIE 5102, 145–155.

Csicsvari, J., Jamieson, B., Wise, K.D., Buzsaki, G., 2003. Mechanisms of gamma oscillations in the hippocampus of the behaving rat. Neuron 37, 311–322.

Di Russo, F., Martinez, A., Sereno, M.I., Pitzalis, S., Hillyard, S.A., 2001. The cortical sources of the early components of the visual evoked potential. Hum. Brain Mapp. 15, 95–111.

Di Russo, F., Pitzalis, S., Spitoni, G., Aprile, T., Patria, F., Spinelli, D., Hillyard, S.A., 2005. Identification of the neural sources of the pattern-reversal VEP. NeuroImage 24, 874–886.

Doiron, B., Longtin, A., Turner, R.W., Maler, L., 2001. Model of gamma frequency burst discharge generated by conditional backpropagation. J. Neurophysiol. 86, 1523–1545.

Eckhorn, R., Gail, A.M., Bruns, A., Gabriel, A., Al-Shaikhli, B., Saam, M., 2005a. Neural mechanisms of visual associative processing. Acta Neurobiol. Exp. (Wars) 64 (2), 239–252.

Eckhorn, R., Gail, A.M., Bruns, A., Gabriel, A., Al-Shaikhli, B., Saam, M., 2005b. Different types of signal coupling in the visual cortex related to neural mechanisms of associative processing and perception. IEEE Trans. Neural Netw. 15, 1039–1052.

Fell, J., Hinrichs, H., Roschke, J., 1997. Time course of human 40 Hz EEG activity accompanying P3 responses in an auditory oddball paradigm. Neurosci. Lett. 235, 121–124.

Fell, J., Klaver, P., Elger, C.E., Fernandez, G., 2002. Suppression of EEG gamma activity may cause the attentional blink. Conscious. Cogn. 11, 114–122.

Friedman-Hill, S., Maldonado, P.E., Gray, C.M., 2000. Dynamics of striate cortical activity in the alert macaque: I. Incidence and stimulus-dependence of gamma-band neuronal oscillations. Cereb. Cortex 10, 1105–1116.

Gruber, W., Klimesch, W., Sauseng, P., Doppelmayr, M., 2005. Alpha phase synchronization predicts P1 and N1 latency and amplitude size. Cereb. Cortex 15, 371–377.

Herrmann, C.S., Mecklinger, A., Pfeifer, E., 1999. Gamma responses and ERPs in a visual classification task. Clin. Neurophysiol. 110, 636–642.

Hurtado, J.M., Rubchinsky, L., Sigvardt, K.A., 2004. Statistical method for detection of phase-locking episodes in neural oscillations. J. Neurophysiol. 91, 1883–1898.

Imas, O.A., Ropella, K.M., Wood, J.D., Hudetz, A.G., 2004. Halothane augments event-related gamma oscillations in rat visual cortex. Neuroscience 123, 269–278.

Jamsek, J., Stefanovska, A., McClintock, P.V.E., Khovanov, I.A., 2003. Time-phase bispectral analysis. Phys. Rev., E. 68, 016201.

Káli, S., Freund, T., 2004. The contributions of different interneuron types to the activity patterns and plasticity of pyramidal cells in the hippocampus. Neurocomputing 58–60, 669–674.

Kalitzin, S., Parra, J., Velis, D., Lopes da Silva, F., 2004. Enhancement of phase clustering in the EEG/MEG gamma frequency band anticipates transition to paroxysmal epileptiform activity in epileptic patients with known visual sensitivity. IEEE Trans. Biomed. Eng. 49 (11), 1279–1286.

Karakas, S., Basar, E., 1998. Early gamma response is sensory in origin: a conclusion based on cross-comparison of results from multiple experimental paradigms. Int. J. Psychophysiol. 31, 13–31.

Karakas, S., Basar-Eroglu, C., Ozesmi, C., Kafadar, H., Erzengin, O.U., 2001. Gamma response of the brain: a multifunctional oscillation that represents bottom-up with top-down processing. Int. J. Psychophysiol. 39, 137–150.

Kayser, C., Konig, P., 2004. Stimulus locking and feature selectivity prevail in complementary frequency ranges of V1 local field potentials. Eur. J. Neurosci. 19, 485–489.

Klimesch, W., Schack, B., Schabus, M., Doppelmayr, M., Gruber, W., Sauseng, P., 2004. Phase-locked alpha and theta oscillations generate the P1–N1 complex and are related to memory performance. Cogn. Brain Res. 19, 302–316.

Krolak-Salmon, P., Henaff, M.-A., Tallon-Baudry, C., Yvert, B., Guenot, M., Vighetto, A., Mauguiere, F., Bertrand, O., 2003. Human lateral geniculate nucleus and visual cortex respond to screen flicker. Ann. Neurol. 53, 73–80.

Kruse, W., Eckhorn, R., 1996. Inhibition of sustained gamma oscillations (35–80 Hz) by fast transient responses in cat visual cortex. Proc. Natl. Acad. Sci. U. S. A. 93, 6112–6117.

Lachaux, J.P., Lutz, A., Rudrauf, D., Cosmelli, D., Quyen, M.L.V., Martinerie, J., Varela, F., 2002. Estimating the time-course of coherence between single-trial brain signals: an introduction to wavelet coherence. Neurophysiol. Clin. 32, 157–174.

Le, J., Menon, V., Gevins, A., 1994. Local estimate of surface Laplacian derivation on a realistically shaped scalp surface and its performance on noisy data. Electroencephalogr. Clin. Neurophysiol. 92, 433–441.

Makeig, S., Westerfield, M., Jung, T.P., Enghoff, S., Townsend, J., Courchesne, E., Sejnowski, T.J., 2002. Dynamic brain sources of visual evoked responses. Science 295, 690–694.

Miranda de Sa, Antonio Mauricio F.L., Catelli Infantosi, Antonio Fernando, 2002. A coherence-based technique for evaluating the degree of synchronism in the EEG during sensory stimulation. Rev. Bras. Eng. Biomed. 18, 39–49.

Morgan, S.T., Hansen, J.C., Hillyard, S.A., 1996. Selective attention to stimulus location modulates the steady-state visual evoked potential. Proc. Natl. Acad. Sci. U. S. A. 93, 4770–4774.

Müller, M.M., Hillyard, S., 2000. Concurrent recording of steady-state and transient event-related potentials as indices of visual-spatial selective attention. Clin. Neurophysiol. 111, 1544–1552.

Müller, M.M., Junghofer, M., Elbert, T., Rochstroh, G., 1997. Visually induced gamma-band responses to coherent and incoherent motion: a replication study. NeuroReport 8, 2575–2579.

Nase, G., Singer, W., Monyer, H., Engel, A.K., 2003. Features of neuronal synchrony in mouse visual cortex. J. Neurophysiol. 90, 1115–1123.

Nunez, P.L., Srinivasan, R., Westdorp, A.F., Wijesinghe, R.S., Tucker, D.M., Silberstein, R.B., Cadusch, P.J., 1997. EEG coherency: I. Statistics, reference electrode, volume conduction, Laplacians, cortical imaging, and interpretation at multiple scales. Clin. Neurophysiol. 103, 499–515.

Oswald, A., Chacron, M., Doiron, B., Bastian, J., Maler, L., 2004. Parallel processing of sensory input by bursts and isolated spikes. J. Neurosci. 24, 4351–4362.

Parra, J., Kalitzin, S.N., Iriarte, J., Blanes, W., Velis, D.N., Lopes da Silva, F.H., 2003. Gamma-band phase clustering and photosensitivity: is there an underlying mechanism common to photosensitive epilepsy and visual perception? Brain 126, 1164–1172.

Regan, David, 1989. Human Brain Electrophysiology. Elsevier, New York.

Rosenblum, M.G., Pikovsky, A.S., Kurths, J., 2004. Synchronization approach to analysis of biological systems. Fluctuation Noise Lett. 4, 53–62.

Samonds, J.M., Bonds, A.B., 2005. Gamma oscillation maintains stimulus structure-dependent synchronization in cat visual cortex. Neurophysiology 93, 223–236.

Sannita, W.G., 2000. Stimulus-specific oscillatory responses of the brain: a time/frequency-related coding process. Clin. Neurophysiol. 111, 565–583.

Sannita, W.G., Bandini, F., Beelke, M., De Carli, F., Carozzo, S., Gesino, D., Mazzella, L., Ogliastro, C., Narici, L., 2001. Time dynamics of stimulus- and event-related gamma band activity: contrast-VEPs and the visual P300 in man. Clin. Neurophysiol. 112, 2241–2249.

Schack, B., Witte, H., Helbig, M., Schelenz, C., Spect, M., 2001. Time-variant non-linear phase-coupling analysis of EEG burst patterns in sedated patients during electroencephalographic burst suppression period. Clin. Neurophysiol. 112, 1388–1399.

Schack, B., Vath, N., Petsche, H., Geissler, H.G., Moller, E., 2002. Phase-coupling of theta–gamma EEG rhythms during short-term memory processing. Int. J. Neurosci. 44, 143–163.

Schanze, T., Eckhorn, R., 1997. Phase correlation among rhythms present at different frequencies: spectral methods, application to microelectrode recordings from visual cortex and functional implications. Int. J. Psychophysiol. 26, 171–189.

Senkowski, D., Herrmann, C.S., 2002. Effects of task difficulty on evoked gamma activity and ERPs in a visual discrimination task. Clin. Neurophysiol. 113, 1742–1753.

Sewards, T.V., Sewards, M.A., 1999. Alpha-band oscillations in visual cortex: part of the neural correlate of visual awareness? Int. J. Psychophysiol. 32, 34–45.

Somogyi, P., Klausberger, T., 2004. Defined types of cortical interneurone structure space and spike timing in the hippocampus. J. Physiol. 562, 9–26.

Spencer, K.M., Nestor, P.G., Niznikiewicz, M.A., Salisbury, D.F., Shenton, M.E., McCarley, R.W., 2003. Abnormal neural synchrony in schizophrenia. J. Neurosci. 23, 7407–7411.

Spencer, K.M., Nestor, P.G., Perlmutter, R., Niznikiewicz, M.A., Klump, M.C., Frumin, M., Shenton, M.E., McCarley, R.W., 2004. Neural synchrony indexes disordered perception and cognition in schizophrenia. Proc. Natl. Acad. Sci. U. S. A. 101, 17288–17293.

Stefanics, G., Jakob, A., Bernath, L., Kellenyi, L., Hemadi, I., 2004. EEG early evoked gamma-band synchronization reflects object recognition in visual oddball tasks. Brain Topogr. 16, 261–264.

Thomson, J., 1982. Spectrum estimation and harmonic analysis. Proc. IEEE 70, 1055–1096.

Tiesinga, P.H.E., Sejnowski, T.J., 2004. Rapid temporal modulation of synchrony by competition in cortical interneuron networks. Neural Comput. 16, 251–275.

Tomberg, C., 1999. Cognitive N140 electrogenesis and concomitant 40 Hz synchronization in mid-dorsolateral prefrontal cortex (area 46) identified in non-averaged human brain potentials. Neurosci. Lett. 266, 141–144.

Tomberg, C., Desmedt, J.E., 1998. Human perceptual processing: inhibition of transient prefrontal parietal 40 Hz binding at P300 onset documented in non averaged cognitive brain potentials. Neurosci. Lett. 255, 163–166.

van Milligen, B.Ph., Sanchez, E., Estrada, T., Hidalgo, C., Branas, B., Carreras, B., Garcia, L., 1995. Wavelet bicoherence: a new turbulence analysis tool. Phys. Plasmas 2, 3017.

van Milligen, B.Ph., Hidalgo, C., Sanchez, E., Pedrosa, M.A., Balbin, R., Garcia-Cortes, I., 1997. Statistically robust linear and nonlinear wavelet analysis applied to plasma edge turbulence. Rev. Sci. Instrum. 68, 967–970.

Volgushev, M., Pernberg, J., Eysel, U.T., 2003. Gamma-frequency fluctuations of the membrane potential and response selectivity in visual cortical neurons. Eur. J. Neurosci. 17, 1768–1776.

Volgushev, M., Pernberg, J., Eysel, U.T., 2004. Response selectivity and gamma-frequency fluctuations of the membrane potential in visual cortical neurons. Neurocomputing 58, 957–963.

von Stein, A., Sarnthein, J., 2000. Different frequencies for different scales of cortical integration: from local gamma to long range alpha/theta synchronization. Int. J. Psychophysiol. 38, 301–313.

von Stein, A., Chiang, C., Koenig, P., 2000. Top-down processing mediated by interareal synchronization. Proc. Natl. Acad. Sci. U. S. A. 97, 14738–14753.

White, J.A., Banks, M.I., Pearce, R.A., Kopell, N.J., 2000. Networks of interneurons with fast and GABAA kinetics provide substrate for mixed gamma–theta rhythm. Proc. Natl. Acad. Sci. U. S. A. 97, 8128–8133.

Whittington, M.A., Traub, R.D., Kopell, N., Ermenttrout, B., Buhl, E.H., 2000. Inhibition-based rhythms: experimental and mathematical observations on network dynamics. Int. J. Psychophysiol. 38, 315–336.